

# 1 Reduced-complexity air quality intervention modelling 2 over China: development of the InMAPv1.6.1-China and 3 comparison with the CMAQv5.2 model

4 Ruili Wu<sup>1,2</sup>, Christopher W. Tessum<sup>3</sup>, Yang Zhang<sup>4</sup>, Chaopeng Hong<sup>5</sup>, Yixuan Zheng<sup>6</sup>,  
5 Qiang Zhang<sup>1</sup>, Xinyin Qin<sup>1</sup>, Shigan Liu<sup>1</sup>

6 <sup>1</sup>Ministry of Education Key Laboratory for Earth System Modelling, Department of Earth System  
7 Science, Tsinghua University, Beijing 100084, China

8 <sup>2</sup>State Environmental Protection Key Laboratory of Quality Control in Environmental Monitoring  
9 China National Environmental Monitoring Centre, Beijing 100012, China

10 <sup>3</sup>Department of Civil and Environmental Engineering, University of Illinois at Urbana-Champaign,  
11 Urbana, Illinois 61801, United States

12 <sup>4</sup>Department of Civil and Environmental Engineering, Northeastern University, Boston, Massachusetts  
13 02115, United States

14 <sup>5</sup>Department of Earth System Science, University of California, Irvine, California 92602, United States

15 <sup>6</sup>Center of Air Quality Simulation and System Analysis, Chinese Academy of Environmental Planning,  
16 Beijing 100012, China

17 Correspondence to: Ruili Wu ([wurl15@tsinghua.org.cn](mailto:wurl15@tsinghua.org.cn) or [wurl@cnemc.cn](mailto:wurl@cnemc.cn))

18 **Abstract.** This paper presents the first development and evaluation of the reduced-complexity air quality  
19 model for China. In this study, a reduced-complexity air quality intervention model over China ( InMAP-  
20 China) is developed by linking a regional air quality model, a reduced-complexity air quality model, an  
21 emission inventory database for China, and a health impact assessment model to rapidly estimate the air  
22 quality and health impacts of emission sources in China. The modelling system is applied over mainland  
23 China for 2017 under various emission scenarios. A comprehensive model evaluation is conducted by  
24 comparison against conventional CMAQ simulations and ground-based observations. We found that  
25 InMAP-China satisfactorily predicted total PM<sub>2.5</sub> concentrations in terms of statistical performance.  
26 Compared with the observed PM<sub>2.5</sub> concentrations, the mean bias (MB), normalized mean bias (NMB),  
27 and correlations of the total PM<sub>2.5</sub> concentrations are -8.1 µg/m<sup>3</sup>, -18%, and 0.6, respectively. The  
28 statistical performance is considered to be satisfactory for a reduced-complexity air quality model and  
29 remains consistent with that evaluated in the United States. The underestimation of total PM<sub>2.5</sub>  
30 concentrations was mainly caused by its composition, primary PM<sub>2.5</sub>. In terms of the ability to quantify  
31 source contributions of PM<sub>2.5</sub> concentrations, InMAP-China presents similar results in comparison with

删除的内容: 2
删除的内容: 3
删除的内容: 4
删除的内容: 5
带格式的: 英语(英国)
带格式的: 上标
带格式的: 字体:(中文) Times New Roman, 10 pt
带格式的: 字体:(中文) Times New Roman, 10 pt
带格式的: 正文, 两端对齐
带格式的: 字体:(中文) Times New Roman, 10 pt
带格式的: 字体:(中文) Times New Roman, 10 pt
带格式的: 字体:(中文) SimSun
删除的内容: 2
删除的内容: 3
删除的内容: 4
删除的内容: 5

40 those based on the CMAQ model, the difference is mainly caused by the different treatment of secondary  
41 inorganic aerosols in the two models. Focusing on the health impacts, the annual PM<sub>2.5</sub>-related premature  
42 mortality estimated using InMAP-China in 2017 was 1.92 million, which was 25 ten thousand deaths  
43 lower than that estimated based on CMAQ simulations as a result of underestimation of PM<sub>2.5</sub>  
44 concentrations. This work presents a version of the reduced-complexity air quality model over China,  
45 provides a powerful tool to rapidly assess the air quality and health impacts associated with control policy,  
46 and to quantify the source contribution attributable to many emission sources.

删除的内容: mechanism and the

## 47 1 Introduction

批注 [吴瑞丽1]: Statement: the revised sentences are marked in red.

48 With rapid urbanization and industrialization, fine particulate matter pollution less than 2.5 μm in  
49 diameter (PM<sub>2.5</sub>) has become a major environmental issue in China. High PM<sub>2.5</sub> concentrations can be  
50 observed over eastern China from satellite observations (Xiao et al., 2020) and the PM<sub>2.5</sub> concentrations  
51 have been largely decreased since 2013 due to the effective control measures taken by Chinese  
52 governments (Zhao et al., 2021). PM<sub>2.5</sub> can affect air quality, ecosystems, and climate change and  
53 damage human health through short-term or long-term exposure. The Global Burden of Disease study  
54 reported that 1.1 million premature deaths were caused by long-term PM<sub>2.5</sub> exposure over China in 2015  
55 (Cohen et al., 2017).

批注 [吴瑞丽2]:

删除的内容: (Xiao et al., 2020) and the PM<sub>2.5</sub> concentrations have been largely decreased since 2013 due to the effective control measures taken by Chinese governments (Zhao et al., 2021)

56 State-of-the-science three-dimensional air quality models (AQMs) have been widely used in China  
57 as tools to simulate regional PM<sub>2.5</sub> concentrations, quantify the contributions to total PM<sub>2.5</sub> concentrations  
58 resulting from emission sources and assess the benefits associated with control measures (Chang et al.,  
59 2019, Li et al., 2015; Zhang et al., 2015; Zhang et al., 2019). The Weather Research and Forecasting  
60 model-Community Multiscale Air Quality Modelling System (WRF-CMAQ) (Appel et al., 2017; Chang  
61 et al., 2019), the Weather Research and Forecasting model coupled with Chemistry (WRF-Chem)  
62 (Reddington et al., 2019), the Weather Research and Forecasting model-Comprehensive Air Quality  
63 Model Extension (WRF-CAMx) (Li et al., 2015), and the Global Adjoint model of Atmospheric  
64 Chemistry (GEOS-Chem Adjoint) (Zhang et al., 2015) were frequently used in previous studies. To  
65 conduct a series of simulations for multiple scenarios or quantify the separate contributions attributable  
66 to multiple sources, large computational resources and run time are required while utilizing conventional  
67 AQMs. To address these challenges, and to improve the availability and accessibility of air quality  
68 modelling, a number of reduced-complexity models have been developed by the air quality research

删除的内容: State-of-the-science three-dimensional air quality models (AQMs)

删除的内容: The Weather Research and Forecasting model-Community Multiscale Air Quality Modelling System (WRF-CMAQ) (Appel et al., 2017; Chang et al., 2019), the Weather Research and Forecasting model coupled with Chemistry (WRF-Chem) (Reddington et al., 2019), the Weather Research and Forecasting model-Comprehensive Air Quality Model Extension (WRF-CAMx) (Li et al., 2015), and the Global Adjoint model of Atmospheric Chemistry (GEOS-Chem Adjoint)

删除的内容: AQMs

删除的内容: these challenges

87 community. The three representative reduced-complexity air quality models frequently used are the  
88 Estimating Air Pollution Social Impacts Using Regression (EASIUR) model (Heo et al., 2016; Heo et  
89 al., 2017), the updated Air Pollution Emission Experiments and Policy (APEEP2) model (Muller et al.,  
90 2007; Muller et al., 2011) and the Intervention for Air Pollution model (InMAP) (Tessum et al., 2017).  
91 A recent study compares three reduced-complexity models, EASIUR, APEEP2, and InMAP, and the  
92 results indicate that these three models are consistent in their assessment of the marginal social cost at  
93 the county level (Gilmore et al., 2019). Reduced-complexity air quality models are less computationally  
94 intensive and easier to use. However, it is not available for China. Therefore, it is essential to develop a  
95 reduced-complexity air quality model over China to quickly predict PM<sub>2.5</sub> concentrations and the  
96 associated health impacts of emission sources.

97 The reduced-complexity intervention model for air pollution, InMAP, was developed by Tessum et  
98 al. (Tessum et al., 2017) to rapidly assess the air pollution, health, and economic impacts resulting from  
99 marginal changes in air pollutant emissions. Compared with conventional air quality models, InMAP has  
100 the advantage of time efficient, can predict annual-average PM<sub>2.5</sub> concentrations within few hours but  
101 with a modest reduction in accuracy compared with CTMs. InMAP reduces the running time by  
102 simplifying the physical and chemical process. InMAP has been used to assess marginal health damage  
103 of location-specific emission sources (Goodkind et al., 2019), to quantify the health impacts of individual  
104 coal-fired power plants in the United States (Thind et al., 2019) and to estimate the health benefits of  
105 control policies considering specific locations (Sergi et al., 2020). However, to date, a version of the  
106 reduced-complexity air quality intervention model over China is absent.

107 In this work, based on the source code of the version 1.6.1 of InMAP model, a reduced-complexity  
108 air quality intervention model over China ( InMAP-China) is developed to rapidly predict the air quality  
109 and estimate the health impacts of emission sources in China. The total consumed time for a simulation  
110 for the year 2017 using the InMAP-China established in this study is approximately an hour with a single  
111 CPU of 24 nodes. Therefore, it is convenient when conducting multiple simulations of PM<sub>2.5</sub>  
112 concentrations due to air pollutants emissions in 2017. The modelling system is applied over mainland  
113 China for 2017 under various emission scenarios to examine model performance. Comparisons against  
114 conventional air quality models and surface observations are performed in this study. The model  
115 applicability and limitations are also declared.

116 The paper is organized as follows: Section 2.1 presents the components of InMAP-China including  
117 the interface development between WRF-CMAQ and InMAP to generate parameters of the base

批注 [吴瑞丽4]:

Line 78: InMAP should be spelled out when it is firstly  
used in the paper.  
Spelled out in Line 80.

带格式的: 下标

删除的内容: including

119 atmospheric state, the preprocessed process of emission input data and the exposure-response functions  
120 employed in this model. Section 2.2 introduces the evaluation protocol, including the statistical variables  
121 adopted and the simulation design in this study. Section 3 presents the evaluation of InMAP-China's  
122 predictions of PM<sub>2.5</sub> air quality and PM<sub>2.5</sub>-related health impacts in several simulations. Section 4  
123 summarizes the conclusions and limitations of this study.

## 124 2 Description of InMAP-China model

### 125 2.1 Model components and configurations

126 The reduced-complexity intervention model for air pollution, InMAP, was developed by Tessum et  
127 al. (Tessum et al., 2017) to rapidly assess the air pollution, health, and economic impacts resulting from  
128 marginal changes in air pollutant emissions. The model has been widely used in studies (Sergi et al.,  
129 2020; Thind et al., 2019; Goodkind et al., 2019; Dimanchevi et al., 2019) focusing on PM<sub>2.5</sub> pollution  
130 and health, economic impacts resulting from emission sources in the United States. In this model, the  
131 continuous equation of atmospheric pollutants is solved at an annual scale, and the run time can be  
132 reduced. The parameters used to represent physical and chemical processes for simplified simulation are  
133 calculated prior to using CTM output data. PM<sub>2.5</sub> air quality and PM<sub>2.5</sub>-related premature mortality are  
134 predicted and output in the InMAP model.

135 In this work, a Chinese version of the reduced-complexity air quality intervention model InMAP-  
136 China is developed for the purpose of rapidly estimating the PM<sub>2.5</sub> concentration and associated health  
137 impacts of emission sources. ~~Figure 1 shows the model framework. Based on the source code of the~~  
138 InMAP model, three-step development work is conducted to establish InMAP-China. First, we develop  
139 a preprocessed interface to calculate physical and chemical process parameters using the WRF-CMAQ  
140 output variables to support the simplified simulation in InMAP-China. Second, air pollutant emission  
141 data are preprocessed to an appropriate format for the InMAP-China simulation. Third, the exposure-  
142 response function of the GEMM model is employed in InMAP-China and replaces the original default  
143 function to assess PM<sub>2.5</sub>-related health impacts.

144 Table 1 presents the basic configurations of InMAP-China. The simulation domain is over East  
145 Asia and covers mainland China. The spatial resolution is 36 km. Fourteen vertical layers are used in  
146 InMAP-China, ranging from the surface layer to the top level of the tropospheric layer.

删除的内容:

删除的内容: Figure 1 shows the model framework.

### 149 2.1.1 Parameter interface development for simplified simulation in InMAP-China

150 We develop a preprocessed interface to calculate physical and chemical process parameters using  
151 WRF-CMAQ output variables for simplified simulation in InMAP-China based on the Environmental  
152 Protection Agency's (EPA) work (Baker et al., 2020). [Two NETCDF files containing the key parameters](#)  
153 [for simplified simulation are generated by using the parameter interface developed here, one is at 36km](#)  
154 [resolution across entire mainland of China and another is at 4km resolution over the BTH region](#). The  
155 main step of the preprocessed interface includes meteorological and chemical variable extraction and  
156 merging, unit conversion, vertical layer mapping, physical and chemical process parameter calculation  
157 and average processing. The hourly chemical and meteorological variable outputs from the WRF-CMAQ  
158 modelling system are converted into annual-average physical and chemical process parameters required  
159 for simplified simulation.

160 A NETCDF file containing the three-dimensional annually averaged parameters to characterize  
161 atmospheric advection, dispersion, mixing, chemical reaction, and deposition is generated. Table 2 shows  
162 the relationship between the annual-average parameters for simplified simulation and the original hourly  
163 variables. In InMAP-China, the annual averaged component and the deviation of wind speed to represent  
164 advection are calculated using hourly elements. The offset of wind vectors in different directions may  
165 result in some uncertainties in this process. The parameters of eddy diffusion and convective transport  
166 are precalculated using hourly elements, including temperature, pressure, boundary layer height, etc. The  
167 annual wet deposition rate is determined by the rainwater mixing ratio and cloud fractions. The annual  
168 dry deposition rate of particles and gaseous pollutants at the surface level is precalculated using friction  
169 speed, heat flux, radiation flux and land cover. ~~The simplification of chemical reactions is different~~  
170 among pollutants. For NO<sub>x</sub>, NH<sub>3</sub>, and volatile organic compound (VOC) precursors, the annual averaged  
171 gas-particle partitioning is adopted and calculated before using the output concentrations of species from  
172 CMAQ. For SO<sub>2</sub> pollutants, the annual oxidation rate of two major conversion pathways for SO<sub>2</sub> is  
173 calculated using concentrations of hydroxyl radical (HO) and hydrogen peroxide (H<sub>2</sub>O<sub>2</sub>) in CMAQ, and  
174 the conversion is estimated in InMAP-China.

### 175 2.1.2 Prior WRF-CMAQ simulation

176 To generate the meteorological and chemical parameters required by InMAP-China, a one-year  
177 WRF-CMAQ simulation [covering the entire mainland of China](#) is conducted to output hourly  
178 meteorological and chemical-related variables in the year 2017. [Besides, the nested WRF-CMAQ](#)

删除的内容: .

带格式的: p1, 两端对齐, 缩进: 首行缩进: 0.63 cm

180 simulation over the BTH region is also conducted and validated using observed data. The corresponded  
181 output data is used to generate the meteorological and chemical parameters required by InMAP-China  
182 for the simulations of 4 km resolution in the BTH region. Tables S1 and S2 show the major configurations  
183 of the WRF-CMAQ modelling system. The WRF model is driven by the National Centers for  
184 Environmental Prediction Final Analysis (NCEP-FNL) (<https://doi.org/10.5065/D6M043C6>) reanalysis  
185 data to provide the initial and boundary conditions. The meteorological fields derived from the WRF  
186 model is used to drive the CMAQ model (Appel et al., 2016) simulations. The air pollutant emissions  
187 used here include anthropogenic emissions over China derived from the MEIC model  
188 (<http://meicmodel.org/>), anthropogenic emissions over the region of East Asia outside China derived  
189 from the MIX-2010 inventory (Li et al., 2015), and biogenic emissions derived from the MEGANv2.10  
190 model. The CB05 chemical mechanism and the AERO6 aerosol module are employed in the model  
191 simulation.

192 Table S3 summarizes the performance statistics of meteorological variables, including surface  
193 temperature, relative humidity, and wind speed, in China in 2017, as simulated by the WRF model. The  
194 hourly observed data of major meteorological variables derived from the National Climate Data Center  
195 (NCDC) are utilized here. The results show that the meteorological variables simulated by the WRF  
196 model agree well with the surface observations, which is consistent with previous studies (Wu et al.,  
197 2019; Zheng et al., 2015; Hong et al., 2017). The model performs well on the predictions of surface  
198 temperature, with an MB of -0.7 K, an NMB of -6.1%, and R of 0.9. The predictions of relative humidity  
199 at a height of 2 metres are relatively satisfied with an MB of 4.1% and an NMB of 6.1%. The predictions  
200 of wind speed at a height of 10 metres are slightly overestimated, with an MB of 0.3 m/s and an NMB  
201 of 12.4%, which may be caused by out-of-date USGS land use data employed in the model runs.

202 The SO<sub>2</sub>, NO<sub>2</sub> and PM<sub>2.5</sub> concentrations modelled across the domain agree well with the surface  
203 observations in terms of the statistical performance and monthly variations. Table S4 summarizes the  
204 performance of the statistics of major air pollutant concentrations. The nationwide annual averaged PM<sub>2.5</sub>  
205 concentration simulated in 2017 in China was 42.1 µg/m<sup>3</sup>. Compared with the observed PM<sub>2.5</sub> of 45.9  
206 µg/m<sup>3</sup>, there are slight underpredictions with an MB of 3.7 µg/m<sup>3</sup> and NMB of 8.1%. The CMAQ model  
207 has moderate underpredictions of the NO<sub>2</sub> concentrations and SO<sub>2</sub> concentrations, which may be related  
208 to the uncertainties of emission inputs. For modelled NO<sub>2</sub> concentrations, MB and NMB are -4.6 µg/m<sup>3</sup>  
209 and -13.9%, respectively. For modelled SO<sub>2</sub> concentrations, MB and NMB are -0.8 µg/m<sup>3</sup> and -4.5%,

210 respectively. Figure S3 shows the monthly variation. The variation trend of the observed SO<sub>2</sub>, NO<sub>2</sub>, and  
211 PM<sub>2.5</sub> concentrations can basically be reproduced in the CMAQ simulations.

### 212 **2.1.3 Preprocessed emission input data**

213 We develop the preprocessed module to generate vector emission input for the InMAP-China  
214 simulation. This module can allocate air pollutant emissions vertically and horizontally to supply the  
215 missing parameters for the emission file and convert them into a shapefile vector format. [The shapefile](#)  
216 [vector format's emission data of 36km resolution in entire mainland of China and 4km resolution in the](#)  
217 [BTH region in 2017 are pre-processed by using this module.](#)

218 In this module, the emission data are preprocessed by source and altitude. The anthropogenic  
219 emissions of five sectors in China in 2017 from the MEIC inventory (<http://meicmodel.org/>), the  
220 anthropogenic emissions over regions outside mainland China in Asia from the MIX-2010 inventory (Li  
221 et al., 2015), and the natural emissions estimated using the MEGANv2.10 model (Guenther et al., 2012)  
222 are employed in this study.

223 More detailed, the gridded anthropogenic emissions of 0.3 degrees for the residential, transportation,  
224 and agricultural sectors are preprocessed and input to the surface layer. The gridded air pollutant  
225 emissions of the industrial sector and noncoal power plants are preprocessed for allocation to attitudes  
226 ranging from 130 metres to 240 metres and 130 metres to 890 metres, respectively. The emissions of  
227 coal-fired power plants (CPPs) are preprocessed as point sources. The air pollutant emissions and the  
228 stack attribution of each unit are provided in the emission file. Because the stack attribution of the power  
229 unit is missed in the MEIC inventory, we supplied the information in the preprocessed module based on  
230 NEI ( National Emission Inventory data) data of power units. For stack height/stack diameter, a linear  
231 relationship is first established (see Figure S1), and then, supplementation for these two parameters of  
232 Chinese power plants is conducted by using the relationships. The fixed value for the other two variables  
233 of stack attribution is set here because the PM<sub>2.5</sub> concentrations attributable to power plants (CPPs-PM<sub>2.5</sub>)  
234 are less sensitive to the two variables (see Figure S2). The stack gas exit velocity and stack gas exit  
235 temperature of the power unit are 6 m/s and 313 K, respectively. The air pollutant emissions over regions  
236 outside mainland China in Asia and the natural emissions simulated by MEGANv2.10 are preprocessed  
237 and input to the surface layer.

删除的内容: .

删除的内容: Additionally, w

删除的内容: T

删除的内容: .

删除的内容: G

删除的内容: .

删除的内容: .

## 245 2.1.4 Exposure-response function from GEMM

246 ~~To rapidly estimate the premature mortality of PM<sub>2.5</sub> exposures,~~ we employ the exposure-response  
247 function from GEMM to estimate PM<sub>2.5</sub>-related premature mortality, which was developed by Burnett  
248 et al. (Burnett et al., 2018), ~~and calculate the premature mortality using PM<sub>2.5</sub> concentration predictions~~  
249 ~~of InMAP-China.~~ Premature mortality due to non-communicable diseases (NCDs) and lower respiratory  
250 infections (LRIs) was considered in this study. Mortality is determined by the mortality incidence rate,  
251 population, and attributable fraction (AF) to certain PM<sub>2.5</sub> concentrations. The national mortality  
252 incidence rate and the population data were derived from the GBD2017 study (Institute for Health  
253 Metrics and Evaluation). The spatial distribution of the population in 2015 from the Gridded Population  
254 of World Version 4 (Doxsey et al., 2015) was employed to allocate the population in 2017.

## 255 2.2 Evaluation protocol

### 256 2.2.1 Evaluation method

257 In this study, the performances of the InMAP-China predictions are evaluated by comparison  
258 against CMAQ simulations and surface observations. Model-to-model comparison and model-to-  
259 observation comparison have both been used to evaluate the performance of reduced-complexity air  
260 quality models in previous studies (Tessum et al., 2017; Gilmore et al., 2019).

261 The following aspects are considered to make an evaluation. First, we examine the ability of  
262 InMAP-China to predict PM<sub>2.5</sub> concentrations at different emission levels, which will be introduced in  
263 Section 3.1. Second, to examine the ability to quantify source contributions to PM<sub>2.5</sub> concentrations, we  
264 compare the InMAP-China's predictions of the sectoral contributions attributable to power, industry,  
265 residential, transportation, and agriculture with those based on the CMAQ model, which will be  
266 presented in Section 3.2. ~~Third, to comprehensively understand the performance at higher spatial~~  
267 ~~resolution using InMAP-China, we compare the predictions of PM<sub>2.5</sub> concentrations at 4km spatial~~  
268 ~~resolution in the BTH region both modelled by InMAP-China and conventional CMAQ with the~~  
269 ~~observations, which is displayed in Section 3.3. Fourth,~~ focusing on the health impacts, the PM<sub>2.5</sub>-related  
270 premature mortality predicted by InMAP-China is also compared with mortality estimation based on  
271 PM<sub>2.5</sub> exposure derived from CMAQ, which is presented in Section 3.4.

272 ~~For the observed PM<sub>2.5</sub> concentration data,~~ the annual averaged observed PM<sub>2.5</sub> concentrations in  
273 2017 were calculated using hourly concentration data from the China National Environmental  
274 Monitoring Center, CNEMC (<http://www.cnemc.cn/>). More than 1400 national monitoring sites for air

删除的内容: In InMAP-China,

带格式的: 下标

带格式的: 下标

带格式的: 下标

删除的内容: Third

删除的内容: 3

已下移 [1]: The statistical parameters used in this study include the correlation coefficient (R), mean bias (MB), mean error (ME), normalized mean bias (NMB), normalized mean error (NME), and root mean square error (RMSE). The statistical analyses on the performance of InMAP-China are similar to our previous evaluation of conventional CTMs (Zheng et al., 2015; Wu et al., 2019).

带格式的: 下标

删除的内容: .

删除的内容: T



287 pollutant concentrations are included in the simulation domain. The statistical parameters used in this  
288 study include the correlation coefficient (R), mean bias (MB), mean error (ME), normalized mean bias  
289 (NMB), normalized mean error (NME), and root mean square error (RMSE). The statistical analyses on  
290 the performance of InMAP-China are similar to our previous evaluation of conventional CTMs ( Zheng  
291 et al., 2015; Wu et al., 2019).

已移动(插入) [1]

## 292 2.2.2 Experimental design

293 We design twelve simulations to examine the model ability of InMAP-China in this study. Table 3  
294 shows the sequence of simulations.

删除的内容: eleven

295 InMAP\_TOT represents the baseline simulation with maximum emissions input, in which five  
296 sectoral anthropogenic emissions are derived from the MEIC inventory, natural emissions are derived  
297 from the MEGANv2.10 model, and Asian emissions outside mainland China are derived from the MIX-  
298 2010 inventory are combined as emission inputs. Five sectoral and five abatement simulations are also  
299 conducted to examine the ability of InMAP-China to predict concentration changes in response to  
300 sectoral emissions and abatement emissions. The emission inputs for these ten simulations have been  
301 declared in Table 3. The annual averaged physical and chemical process parameters are calculated based  
302 on the output variables of WRF-CMAQ model, which has already been mentioned in Section 2.1.2.  
303 Based on the above input, the particle continuity equations are solved by InMAP-China model to obtain  
304 the annual averaged PM<sub>2.5</sub> concentrations at the steady-state of the atmosphere. The above simulations  
305 are all conducted at 36km spatial resolution across the entire mainland of China. Besides, another  
306 simulation represented by InMAP-BTH is conducted at 4km spatial resolution over the BTH region, with  
307 the anthropogenic emission input data at 4km resolution derived from the MEIC inventory and natural  
308 emissions derived from the MEGANv2.10 model is utilized in this simulation.

删除的内容:

309 In order to make a comparison with the InMAP-China simulations, eleven CMAQ simulations are  
310 also performed under the same emission inputs. The hourly PM<sub>2.5</sub> concentrations simulated by CMAQ  
311 in 2017 are averaged at obtain the annual averaged PM<sub>2.5</sub> concentrations. Due to limited computational  
312 resources, each simulation is conducted for four representative months (January, April, July, and October)  
313 in 2017.

删除的内容: Five sectoral and five abatement simulations are also conducted to examine the ability of InMAP-China to predict concentration changes in response to sectoral emissions and abatement emissions. The emission inputs for these ten simulations have been declared in Table 3. The annual averaged physical and chemical process parameters are calculated based on the output variables of WRF-CMAQ model, which has already been mentioned in Section 2.1.2. Based on the above input, the particle continuity equations are solved by InMAP-China model to obtain the annual averaged PM<sub>2.5</sub> concentrations at the steady state of atmosphere.

## 328 3 Results and Discussion

### 329 3.1 Model performance of PM<sub>2.5</sub> concentrations in China

#### 330 3.1.1 Total PM<sub>2.5</sub> concentrations

331 Figure 3 shows the performance evaluation of total PM<sub>2.5</sub> concentrations in the InMAP\_TOT  
332 simulations. Compared with the observed annual averaged PM<sub>2.5</sub> concentrations, the total PM<sub>2.5</sub>  
333 concentrations are moderately underpredicted by InMAP-China with an MB of -8.1 μg/m<sup>3</sup> and an NMB  
334 of -18.1%. Compared with the CMAQ predictions, the total PM<sub>2.5</sub> concentrations are also underpredicted,  
335 with an MB of -5.3 μg/m<sup>3</sup> due to the underprediction of primary PM<sub>2.5</sub>. Consistent air pollutant emissions  
336 are employed in the CMAQ and InMAP-China simulations. Therefore, the underpredictions are caused  
337 by the different mechanisms in the two models. Basically, InMAP-China reproduces the spatial pattern  
338 of total PM<sub>2.5</sub> concentrations simulated by CMAQ. Notably, significant overpredictions of PM<sub>2.5</sub>  
339 concentrations can be observed over mountain areas across Northern China, and the complex terrain and  
340 large emission intensity increase the challenge of predicting PM<sub>2.5</sub> concentrations using the reduced-  
341 complexity air quality model in this region.

342 Figure 4 shows a comparison of PM<sub>2.5</sub> compositions. Compared with the CMAQ results, the  
343 InMAP-China predictions of PM<sub>2.5</sub> compositions are satisfactory, with NMBs for SO<sub>4</sub><sup>2-</sup>, NO<sub>3</sub><sup>-</sup>, NH<sub>4</sub><sup>+</sup>, and  
344 primary PM<sub>2.5</sub> equal to 13%, -8%, -10%, and -23%, respectively. The predictions of SO<sub>4</sub><sup>2-</sup>, NO<sub>3</sub><sup>-</sup>, and  
345 NH<sub>4</sub><sup>+</sup> perform better than those of primary PM<sub>2.5</sub>. Figure 5 and Figure 6 compare the spatial distribution  
346 of PM<sub>2.5</sub> compositions, and similar over-predictions of PM<sub>2.5</sub> compositions can be observed in the  
347 mountain area in Northern China.

348 The ability of InMAP-China to predict PM<sub>2.5</sub> compositions is also examined at various emission  
349 levels. Figure 7 compares the concentrations of PM<sub>2.5</sub> compositions and the proportions of secondary  
350 inorganic aerosols (hereafter, SNA) in total PM<sub>2.5</sub> concentrations in different scenarios by two models.  
351 In the InMAP\_TOT scenario, the proportion of SNA is 56%, which is extremely close to the 50%  
352 proportion in the WRF-CMAQ simulations. In five emission abatement simulations, the proportion was  
353 approximately equal to that in the baseline scenario because the linearly treated chemical reaction  
354 relationship of SNA was employed in InMAP-China. However, focusing on the simulations of five  
355 sectoral emission scenarios, a significant difference can be observed, which is mainly caused by the  
356 difference in chemical treatments in InMAP-China and CMAQ. In this situation, the impacts on PM<sub>2.5</sub>  
357 concentrations are distinct due to the nonlinear emission-concentration process.

### 358 3.1.2 Marginal change in PM<sub>2.5</sub> concentrations

359 Figure 8 compares the InMAP-China and CMAQ predictions of population-weighted PM<sub>2.5</sub>  
360 concentrations and PM<sub>2.5</sub> compositions for eleven emission scenarios. Marginal changes in air pollutant  
361 concentrations are defined as 1 µg/m<sup>3</sup> by normalizing the population-weighted air pollutant  
362 concentrations of each scenario using the largest value among all scenarios modelled by CMAQ. The  
363 InMAP-China reproduces CMAQ predictions on the marginal change in population-weighted PM<sub>2.5</sub>  
364 concentrations, with a NMB of -12% and correlations of 0.98, as shown in Figure 8(a). This performance  
365 is similar to that predicted by InMAP in the United States (Tessum et al., 2017).

366 Figure 8(b)-(f) compares the predictions of PM<sub>2.5</sub> compositions. The InMAP-China predictions of  
367 SO<sub>4</sub><sup>2-</sup>, NO<sub>3</sub><sup>-</sup>, NH<sub>4</sub><sup>+</sup> and primary PM<sub>2.5</sub> agree well with the CMAQ results, but the predictions of secondary  
368 organic aerosol (SOA) are the poorest. The marginal changes in NO<sub>3</sub><sup>-</sup> and primary PM<sub>2.5</sub> concentrations  
369 are moderately underpredicted by InMAP-China, with NMB values of -13% and -21%, respectively.  
370 Conversely, the marginal change in SO<sub>4</sub><sup>2-</sup> concentrations is overpredicted with an NMB of 23%. The  
371 marginal change in NH<sub>4</sub><sup>+</sup> predicted by InMAP-China agrees well with the CMAQ predictions. Because  
372 few reaction pathways of SOA are included in the CB05 mechanism in the CMAQ simulations, SOAs  
373 are underpredicted in the entire modelling system.

374 The regional performance of the changes in PM<sub>2.5</sub> and its compositions for eleven emission  
375 scenarios is also examined in this study. Figures S4-S7 show the regional results. Four regions, including  
376 the Beijing-Tianjin-Hebei region (\_BTH), Yangtze River Delta (\_YRD), Pearl River Delta (\_PRD), and  
377 Fen Wei Plain (\_FWP), are analysed here (see Figure 2). At the regional level, the CMAQ predicted  
378 marginal changes in population-weighted PM<sub>2.5</sub> concentrations, and its composition can be reproduced  
379 by InMAP-China, which is similar to the nationwide performance. However, the marginal change in  
380 SO<sub>4</sub><sup>2-</sup> concentrations over the BTH is significantly overpredicted by InMAP-China, with an NMB of  
381 135%, which is expected to be improved by optimizing the representation of the annual sulfate oxidation  
382 rate in this region.

### 383 3.2 Model performance of source contributions in China

384 Figure 9 shows the contribution of each sector to PM<sub>2.5</sub> concentrations nationwide and at the regional  
385 scale, and Table 4 displays the proportion value of sectoral contribution based on two models. The  
386 predictions of the source contributions of PM<sub>2.5</sub> concentrations in InMAP-China are basically reliable  
387 compared with those based on the CMAQ model, and the difference can be explained.

388 The results based on the two models indicate that the industrial and residential sectors are the first  
389 and second contributors among the five sectors. The contribution of the electricity sector is comparable  
390 when using the two models, while the contributions of transportation and agriculture are moderately  
391 different, which is mainly due to the difference in the model mechanism and the treatment of secondary  
392 inorganic aerosols in the two models. At the regional scale, the difference in the sectoral contribution  
393 caused by the mechanism in the two models is more significant than at the national scale.

### 394 3.3 Model performance of PM<sub>2.5</sub> predictions at higher resolution in the BTH region

395 We also conducted a simulation with higher spatial resolution of 4 km in the BTH region by using  
396 InMAP-China model and make a comparison with the WRF-CMAQ nested simulation at the same area  
397 in the BTH region. Figure 10 and Figure 11 show the performance evaluation of total PM<sub>2.5</sub> concentration  
398 and the composition in the InMAP BTH scenario. Compared with the observed annual averaged PM<sub>2.5</sub>  
399 concentrations, the total PM<sub>2.5</sub> concentrations are moderately overpredicted in InMAP BTH with an  
400 NMB of 41.3% and an R of 0.5.

401 Further compared with the nested CMAQ predictions, the total PM<sub>2.5</sub> concentrations are also over-  
402 predicted by InMAP-China model. The predictions of PM<sub>2.5</sub> compositions in the InMAP BTH scenario  
403 are partially satisfactory, except for SO<sub>4</sub><sup>2-</sup>, with NMBs for SO<sub>4</sub><sup>2-</sup>, NO<sub>3</sub><sup>-</sup>, NH<sub>4</sub><sup>+</sup>, and primary PM<sub>2.5</sub> equal  
404 to 178%, 36%, 33%, and 27%, respectively. Figure 12 further shows the comparison of the spatial  
405 distribution of PM<sub>2.5</sub> compositions in the BTH region. The overall spatial distribution pattern of PM<sub>2.5</sub>  
406 compositions is similarly modeled by two models, however, an obvious difference can be observed  
407 across the mountain area in the BTH region, for instance, the over-predictions of PM<sub>2.5</sub> compositions,  
408 especially, SO<sub>4</sub><sup>2-</sup> and NO<sub>3</sub><sup>-</sup> observed near the Taihang mountain area.

### 409 3.4 Model performance of PM<sub>2.5</sub>-related premature mortality in China

410 To examine the performance of the predictions of PM<sub>2.5</sub>-related premature mortality, a comparison  
411 of premature mortality using the PM<sub>2.5</sub> predictions from InMAP-China and CMAQ, separately, is  
412 performed here. Figure 13 shows the comparison based on two models for all provinces. The results  
413 demonstrate that, compared with the premature mortality based on CMAQ, the relative difference is  
414 ranging from -44% to 15% at the provincial level due to the difference of PM<sub>2.5</sub> concentrations in the two  
415 models.

416 At the provincial level, the PM<sub>2.5</sub>-related premature mortality in Beijing city, Tianjin city, Hebei  
417 province, and Shanghai city is slightly over-predicted by InMAP-China, with the relative difference

删除的内容: 3.3 Model performance of PM2.5-related premature mortality .  
We also conducted

带格式的: 字体:(默认) Times New Roman, (中文) Times New Roman, 字体颜色: 自动

带格式的: 标题 2, 缩进: 首行缩进: 0 cm, 空格段前: 12 磅, 段后: 12 磅, 行距: 单线

带格式的: 非 上标/ 下标

带格式的: 字体:Times New Roman, 下标

带格式的: 字体:Times New Roman

带格式的: 字体:10 pt, 非 斜体

带格式的: 字体:非 斜体

带格式的: 字体:(中文) +中文主题正文 (DengXian)

带格式的: 下标

421 ranging from 4% to 15%. Conversely, for the other majority of provinces, PM<sub>2.5</sub>-related premature  
422 mortality is under-predicted by InMAP-China, with the relative difference ranging from -3% to -44%.  
423 Overall, the PM<sub>2.5</sub>-related premature mortality estimated using InMAP-China was 1.92 million people in  
424 2017. Compared with the CMAQ-based estimations, 25 ten thousand deaths are under-predicted by  
425 InMAP-China because of underestimation of total PM<sub>2.5</sub> concentrations in the baseline simulation.

#### 426 4 Conclusions

427 This work develops a reduced-complexity air quality intervention model over China and presents a  
428 comprehensive evaluation by comparing CMAQ simulations and surface observations. The InMAP-  
429 China aims at providing a simplified modeling tool to rapidly predict the PM<sub>2.5</sub> concentrations due to  
430 emission change as well as health impact of emission sources in China. After the model is established,  
431 the total consumed time for a new simulation under the atmosphere condition in the year 2017 across the  
432 mainland of China using InMAP-China is merely an hour with a single CPU of 24 nodes. Therefore, it  
433 is time-efficient when conduct new simulations of PM<sub>2.5</sub> concentrations in China. Notably, the running  
434 of WRF-CMAQ simulations is merely necessary in our developing stage of InMAP-China. For the  
435 application of InMAP-China, we recommend users to select InMAP-China as a prior tool with extensive  
436 simulation demands, for instance, to quantify the PM<sub>2.5</sub> concentrations due to hundreds of pollution  
437 emitters or to rapidly estimate the PM<sub>2.5</sub> concentrations caused by dozens of control policies, separately.  
438 Besides, the variable grid can also be set in InMAP-China to allow high spatial resolution of 1 km or even  
439 higher in certain urban area.

440 InMAP-China has moderately satisfactory performance in this study, however, this model has  
441 reductions in accuracy compared with conventional CTMs. Overall, InMAP-China satisfactorily predicts  
442 total PM<sub>2.5</sub> concentrations in the baseline simulation in terms of statistical performance. Compared with  
443 the observed PM<sub>2.5</sub> concentrations, the MB, NMB, and correlations of the total PM<sub>2.5</sub> concentrations are  
444 -8.1 µg/m<sup>3</sup>, -18%, and 0.6, respectively. The statistical performance is satisfactory for a reduced-  
445 complexity air quality model and remains consistent with the performance evaluation in the United States.  
446 The underestimation of total PM<sub>2.5</sub> mainly comes from the primary PM<sub>2.5</sub>. Moreover, the spatial pattern  
447 of total PM<sub>2.5</sub> concentrations can be reproduced in InMAP-China, while an overestimation over the  
448 mountain area in Northern China can be observed. The large emission intensity and complex terrain over  
449 this region increase the difficulty of modelling concentrations in this area. The predictions of source  
450 contributions to PM<sub>2.5</sub> concentrations by InMAP-China are comparable with those based on the CMAQ

删除的内容:

带格式的: 缩进: 首行缩进: 0.71 cm

删除的内容: InMAP-China has the advantage of being time-efficient in conducting air quality predictions and health impact assessments of emission sources in China.

带格式的: 字体:10 pt, 非 斜体, 字体颜色: 文字 1

带格式的: 下标

带格式的: 下标

删除的内容: InMAP-China performed well for the prediction of PM<sub>2.5</sub> concentrations. The

删除的内容: model

458 model, and the difference is mainly caused by the uncertainty of the simplification of chemical process  
459 in the InMAP-China. The global version of reduced-complexity air quality model ( Global-InMAP) is  
460 also developed and preprint recently ( Thakrar et al., 2021), our results of InMAP-China can provide  
461 more accurate result in the mainland of China.

462 This study is subject to some limitations and uncertainties. In InMAP-China, the annual-average  
463 chemical and physical processes parameters are calculated using hourly parameters from WRF-CMAQ.  
464 Complicated seasonal and daily variations affecting the formation and transportation of particulate matter  
465 are challenging to retain. The intensity of advection of the air mass is supposed to be weakened due to  
466 the offset of the wind vector in the averaging process, which was also pointed out in a previous study.  
467 Moreover, InMAP-China has difficulty predicting SOA concentrations because reaction pathways for  
468 SOA are insufficient in this modelling system. Further research work is suggested to improve the model  
469 performance. For instance, the combination of machine learning with the simplified simulation may need  
470 to research to promote the reduced-complexity air quality modeling over China.

471  
472

473  
474  
475  
476  
477  
478  
479  
480  
481  
482  
483  
484

**删除的内容:** Focusing on the predictions of health impacts, InMAP-China shows moderate under-predictions of 25 ten thousand people deaths compared with CMAQ-based predictions due to the underestimation of total PM<sub>2.5</sub> concentrations.

**删除的内容:** Although the modelling system has an acceptable performance, research work is suggested to further improve the model performance. This study is subject to some limitations and uncertainties. In InMAP-China, the annual-average chemical and physical processes parameters are calculated using hourly parameters from WRF-CMAQ. Complicated seasonal and daily variations affecting the formation and transportation of particulate matter are challenging to retain. The intensity of advection of the air mass is supposed to be weakened due to the offset of the wind vector in the averaging process, which was also pointed out in a previous study. Moreover, InMAP-China has difficulty predicting SOA concentrations because reaction pathways for SOA are insufficient in this modelling system. . Instead, if the objective of simulations is to predict the actual situation and pre-estimate the reductions in PM<sub>2.5</sub> concentrations due to control measures, conventional CTMs are a better choice because the change in atmospheric conditions along with emission change should be taken into account.

已移动(插入) [2]

**删除的内容:** Instead, if the objective of simulations is to predict the actual situation and pre-estimate the reductions in PM<sub>2.5</sub> concentrations due to control measures, conventional CTMs are a better choice because the change in atmospheric

**带格式的:** 缩进: 首行缩进: 0.71 cm

**带格式的:** 字体: 10 pt

**带格式的:** 英语(美国)

**带格式的:** 缩进: 首行缩进: 0 cm

**已上移 [2]:** In terms of the applicability of this modelling system, we recommend users to select InMAP-China as a

**删除的内容:** The development of InMAP-China aims at providing an alternative to the conventional CTMs to

**带格式的:** 字体: (中文) SimSun, 字体颜色: 文字 1, 英语(美国)

**带格式的:** 字体: (中文) SimSun, 英语(美国)

**带格式的:** 字体: (中文) SimSun, 10 pt, 英语(美国)

**删除的内容:** Code and data availability .

561 **Code and data availability**  
562 The source code for the localized version of reduced-complexity air quality model over China ( InMAP-  
563 China), which is developed based on the original InMAP model over the United states. The data related  
564 to this study as well as the user manual are available at <https://doi.org/10.5281/zenodo.5111961>.

带格式的: 标题 1, 左对齐, 空格 段前: 24 磅, 段后: 12 磅, 行距: 单线  
带格式的

565 **Author contributions**  
566 RL. Wu and Q. Zhang designed the research and RL. Wu carried them out. RL. Wu, CW. Tessum and  
567 Y. Zhang contributed to model development. RL. Wu prepared the manuscript with contributions from  
568 all co-authors.

删除的内容: The source code for the localized version of reduced-complexity air quality model over China ( InMAP-China), which is developed based on the original InMAP model over the United states. The data related to this study as well as the user manual are available at <https://doi.org/10.5281/zenodo.5111961>.

569 **Competing interests**  
570 The authors declare no competing interests.

571 **Acknowledgements**  
572 This work was supported by the National Natural Science Foundation of China (41921005 and  
573 41625020). And this work was also funded under Assistance Agreement No. RD835871 awarded by the  
574 U.S. EPA to Yale University. The views expressed in this manuscript are those of the authors alone and  
575 do not necessarily reflect the views and policies of the U.S. EPA. The EPA does not endorse any products  
576 or commercial services mentioned in this publication.

577  
578  
579  
580  
581  
582  
583  
584  
585  
586

删除的内容:  
带格式的: 左对齐, 行距: 单线  
带格式的: 字体:(中文)+中文主题正文 (DengXian), 小四, 字体颜色: 自动  
删除的内容:

带格式的: 字体:(中文)+中文主题正文 (DengXian), 小四, 字体颜色: 自动

595 **References**

- 596 A. Xiu, J. E. Pleim. Development of a Land Surface Model. Part I: Application in a Mesoscale  
597 Meteorological Model. *Journal of Applied Meteorology*, 40:192-209, 2011.
- 598 Appel, K.W., Napelenok, S.L., Hogrefe, C., Foley, K.M., Pouliot, G.A., Murphy, B., Heath, N., Roselle,  
599 S., Pleim, J., Bash, J.O., Pye, H.O.T., Mathur, R. Overview and evaluation of the Community Multiscale  
600 Air Quality (CMAQ) modelling system version 5.2. *Air Pollution Modelling and its Application XXV*,  
601 11:63-72. ITM 2016. Springer Proceedings in Complexity. Springer, Cham, doi: 10.1007/978-3-319-  
602 57645-9\_11, 2017.
- 603 Appel, K.W., Napelenok, S.L., Hogrefe, C., Foley, K.M., Pouliot, G.A., Murphy, B., Heath, N., Roselle,  
604 S., Pleim, J., Bash, J.O., Pye, H.O.T., Mathur, R. Overview and evaluation of the Community Multiscale  
605 Air Quality (CMAQ) modelling system version 5.2. *Air Pollution Modelling and its Application XXV*,  
606 11:63-72. ITM 2016. Springer Proceedings in Complexity. Springer, Cham, doi: 10.1007/978-3-319-  
607 57645-9\_11, 2017.
- 608 Baker, K. R.; Amend, M.; Penn, S.; Bankert, J.; Simon, H.; Chan, E.; Fann, N.; Zawacki, M.; Davidson,  
609 K.; Roman, H., A database for evaluating the InMAP, APEEP, and EASIUR reduced complexity air-  
610 quality modelling tools. *Data in Brief*, 28, 2020.
- 611 Burnett, R.; Chen, H.; Szyszkowicz, M.; Fann, N.; Hubbell, B.; Pope, C. A.; Apte, J. S.; Brauer, M.;  
612 Cohen, A.; Weichenthal, S.; Coggins, J.; Di, Q.; Brunekreef, B.; Frostad, J.; Lim, S. S.; Kan, H. D.;  
613 Walker, K. D.; Thurston, G. D.; Hayes, R. B.; Lim, C. C.; Turner, M. C.; Jerrett, M.; Krewski, D.; Gapstur,  
614 S. M.; Diver, W. R.; Ostro, B.; Goldberg, D.; Crouse, D. L.; Martin, R. V.; Peters, P.; Pinault, L.;  
615 Tjepkema, M.; Donkelaar, A.; Villeneuve, P. J.; Miller, A. B.; Yin, P.; Zhou, M. G.; Wang, L. J.; Janssen,  
616 N. A. H.; Marra, M.; Atkinson, R. W.; Tsang, H.; Thach, Q.; Cannon, J. B.; Allen, R. T.; Hart, J. E.;  
617 Laden, F.; Cesaroni, G.; Forastiere, F.; Weinmayr, G.; Jaensch, A.; Nagel, G.; Concin, H.; Spadaro, J.  
618 V., Global estimates of mortality associated with long-term exposure to outdoor fine particulate matter.  
619 *Proceedings of the National Academy of Sciences of the United States of America*, 115, (38), 9592-9597,  
620 2018.
- 621 C. J. Walcek, Taylor GR. A Theoretical Method for Computing Vertical Distributions of Acidity and  
622 Sulfate Production within Cumulus Clouds. *Journal of the Atmospheric Science*, 43:339-55, 1986.

删除的内容:

A. Xiu, J. E. Pleim. Development of a Land Surface Model.

删除的内容: Journal of the Atmospheric Science



626 Chang, X.; Wang, S.; Zhao, B.; Xing, J.; Liu, X.; Wei, L.; Song, Y.; Wu, W.; Cai, S.; Zheng, H.; Ding,  
627 D.; Zheng, M., Contributions of inter-city and regional transport to PM<sub>2.5</sub> concentrations in the Beijing-  
628 Tianjin-Hebei region and its implications on regional joint air pollution control. *Science of the Total*  
629 *Environment*, 660, 1191-1200, 2019.

630 Cohen, A. J.; Brauer, M.; Burnett, R.; Anderson, H. R.; Frostad, J.; Estep, K.; Balakrishnan, K.;  
631 Brunekreef, B.; Dandona, L.; Dandona, R.; Feigin, V.; Freedman, G.; Hubbell, B.; Jobling, A.; Kan, H.;  
632 Knibbs, L.; Liu, Y.; Martin, R.; Morawska, L.; Pope, C. A., III; Shin, H.; Straif, K.; Shaddick, G.; Thomas,  
633 M.; van Dingenen, R.; van Donkelaar, A.; Vos, T.; Murray, C. J. L.; Forouzanfar, M. H., Estimates and  
634 25-year trends of the global burden of disease attributable to ambient air pollution: an analysis of data  
635 from the Global Burden of Diseases Study 2015. *Lancet* 389, (10082), 1907-1918, 2017.

636 Dimanchevi, E. G.; Paltsev, S.; Yuan, M.; Rothenberg, D.; Tessum, C. W.; Marshall, J. D.; Selin, N. E.,  
637 Health co-benefits of sub-national renewable energy policy in the US. [Environmental Research Letters](#),  
638 14, (8), 2019.

639 Doxsey-Whitfield E, MacManus K, Adamo S B, Susana B, Pistolesi L, Squires J, Borkovska O and  
640 Baptista S R Taking advantage of the improved availability of census data: a first look at the gridded  
641 population of the world, version 4. *Papers in Applied Geography*. 1 226–34, 2015.

642 E. J. Mlawer, S. J. Taubman, P. D. Brown, M. J. Iacono, S. A. Clough. Radiative transfer for  
643 inhomogeneous atmospheres: RRTM, a validated correlated-k model for the longwave. [Journal of](#)  
644 [Geophysical Research](#), 102:16663-82, 1997.

645 Fountoukis C and Nenes A. ISORROPIA II: A Computationally Efficient Aerosol Thermodynamic  
646 Equilibrium Model for K<sup>+</sup>, Ca<sup>2+</sup>, Mg<sup>2+</sup>, NH<sub>4</sub><sup>+</sup>, Na<sup>+</sup>, SO<sub>4</sub><sup>2-</sup>, NO<sub>3</sub><sup>-</sup>, Cl<sup>-</sup>, H<sub>2</sub>O Aerosols, [Atmospheric](#)  
647 [Chemistry Physics](#), 7, 4639-4659, 2007.

648 Gilmore, E. A.; Heo, J.; Muller, N. Z.; Tessum, C. W.; Hill, J. D.; Marshall, J. D.; Adams, P. J., An inter-  
649 comparison of the social costs of air quality from reduced-complexity models. *Environmental Research*  
650 *Letters*, 14, (7), 2019.

651 Global Burden of Disease Collaborative Network. Global Burden of Disease Study 2017 (GBD 2017)  
652 Population Estimates 1950-2017. Seattle, United States: Institute for Health Metrics and Evaluation  
653 (IHME), 2018.

删除的内容: Environmental Research Letters

删除的内容: Journal of Geophysical Research

删除的内容: Atmospheric Chemistry Physics

657 Global Burden of Disease Collaborative Network. Global Burden of Disease Study 2017 (GBD 2017)  
658 Cause-Specific Mortality 1980-2017. Seattle, United States: Institute for Health Metrics and Evaluation  
659 (IHME), 2018.

660 Goodkind AL, Tessum CW, Coggins JS, Hill JD, Marshall JD. Fine-scale damage estimates of particulate  
661 matter air pollution reveal opportunities for location-specific mitigation of emissions. Proceedings of the  
662 National Academy of Sciences. Apr 3:201816102. <https://doi.org/10.1073/pnas.1816102116>, 2019.

663 Guenther, A. B.; Jiang, X.; Heald, C. L.; Sakulyanontvittaya, T.; Duhl, T.; Emmons, L. K.; Wang, X.,  
664 The Model of Emissions of Gases and Aerosols from Nature version 2.1 (MEGAN2.1): an extended and  
665 updated framework for modelling biogenic emissions. Geoscientific Model Development Discussions,  
666 5, (2), 1503-1560, 2012.

667 Heo, J.; Adams, P. J.; Gao, H. O., Public health costs accounting of inorganic PM<sub>2.5</sub> pollution in  
668 metropolitan areas of the United States using a risk-based source-receptor model. Environment  
669 International, 106, 119-126, 2017.

670 Heo, J.; Adams, P. J.; Gao, H. O., Reduced-form modelling of public health impacts of inorganic PM<sub>2.5</sub>  
671 and precursor emissions. Atmospheric Environment, 137, 80-89, 2016.

672 Hong, C.; Zhang, Q.; Zhang, Y.; Tang, Y.; Tong, D.; He, K., Multi-year downscaling application of two-  
673 way coupled WRF v3.4 and CMAQ v5.0.2 over east Asia for regional climate and air quality modelling:  
674 model evaluation and aerosol direct effects. Geoscientific Model Development, 10, (6), 2447-2470, 2017.

675 J. E. Pleim. A Combined Local and Nonlocal Closure Model for the Atmospheric Boundary Layer. Part  
676 I: Model Description and Testing. Journal of Applied Meteorology and Climatology, 46:1383-95, 2007.

677 J. S. Chang, R. A. Brost, I. S. A. Isaksen, S. Madronich, P. Middleton, W. R. Stockwell, et al. A three-  
678 dimensional Eulerian acid deposition model: Physical concepts and formulation. [Journal of Geophysical](#)  
679 [Research](#), 92:14681-700, 1987.

680 J. S. Kain. The Kain-Fritsch Convective Parameterization: An Update. Journal of Applied Meteorology.  
681 2004, 43:170-81.

682 Li, M.; Zhang, Q.; Kurokawa, J.-i.; Woo, J.-H.; He, K.; Lu, Z.; Ohara, T.; Song, Y.; Streets, D. G.;  
683 Carmichael, G. R.; Cheng, Y.; Hong, C.; Huo, H.; Jiang, X.; Kang, S.; Liu, F.; Su, H.; Zheng, B., MIX:  
684 a mosaic Asian anthropogenic emission inventory under the international collaboration framework of the

删除的内容: Journal of Geophysical Research

686 MICS-Asia and HTAP. *Atmospheric Chemistry and Physics*, 17, (2), 935-963, 2017.

687 Li, X.; Zhang, Q.; Zhang, Y.; Zheng, B.; Wang, K.; Chen, Y.; Wallington, T. J.; Han, W.; Shen, W.; Zhang,  
688 X.; He, K., Source contributions of urban PM<sub>2.5</sub> in the Beijing-Tianjin-Hebei region: Changes between  
689 2006 and 2013 and relative impacts of emissions and meteorology. *Atmospheric Environment*, 123, 229-  
690 239, 2015.

691 Liu, F.; Zhang, Q.; Tong, D.; Zheng, B.; Li, M.; Huo, H.; He, K. B., High-resolution inventory of  
692 technologies, activities, and emissions of coal-fired power plants in China from 1990 to 2010.  
693 *Atmospheric Chemistry and Physics*, 15, (23), 13299-13317, 2015.

694 M.-D. Chou, M. J. Suarez, C.-H. Ho, M. M.-H. Yan, K.-T. Lee. Parameterizations for Cloud Overlapping  
695 and Shortwave Single-Scattering Properties for Use in General Circulation and Cloud Ensemble Models.  
696 *Journal of Climate*, 11:202-14, 1998.

697 Muller, N. Z., Mendelsohn, R. Measuring the damages of air pollution in the United States. *Journal of*  
698 *Environmental Economics and Management*, 54(1), 1–14. <https://doi.org/10.1016/j.jeem.2006.12.002>,

699 Muller, N. Z., Mendelsohn, R., & Nordhaus, W. Environmental accounting for pollution in the United  
700 States economy. *American Economic Review*, 101(5), 1649-75. DOI:10.1257/aer.101.5.1649, 2011.

701 Multi-resolution Emission Inventory of China ( <http://meicmodel.org/>).

702 National Centers for Environmental Prediction/National Weather Service/NOAA/US Department of  
703 Commerce NCEP FNL Operational Model Global Tropospheric Analyses, continuing from July 1999  
704 Dataset (<https://doi.org/10.5065/D6M043C6>), 2000.

705 Reddington, C. L.; Conibear, L.; Knote, C.; Silver, B.; Li, Y. J.; Chan, C. K.; Arnold, S. R.; Spracklen,  
706 D. V., Exploring the impacts of anthropogenic emission sectors on PM<sub>2.5</sub> and human health in South and  
707 East Asia. *Atmospheric Chemistry and Physics*, 19, (18), 11887-11910, 2019.

708 Sergi, B. J.; Adams, P. J.; Muller, N. Z.; Robinson, A. L.; Davis, S. J.; Marshall, J. D.; Azevedo, I. L.,  
709 Optimizing Emissions Reductions from the U.S. Power Sector for Climate and Health Benefits.  
710 *Environmental science & technology*, 54, (12), 7513-7523, 2020.

711 Skamarock W, Klemp J, Dudhia J, Gill D, Barker D, Duda M, Huang X, Wang Wand Powers J A  
712 description of the Advanced Research WRF Version 3 NCAR technical note ( Boulder, CO: National  
713 Center for Atmospheric Research), 2008.

714 Tessum, C. W.; Hill, J. D.; Marshall, J. D., InMAP: A model for air pollution interventions. PLoS One,  
715 12, (4), e0176131, 2017.

716 ~~Thakrar S. T.; Tessum C. W.; Apte J. S.; Balasubramanian S.; Millet D. B.; Pandis S. N.; Marshall J. D.~~  
717 ~~Hill J. D., et al. Global, High-Resolution, Reduced-Complexity Air Quality Modeling Using InMAP~~  
718 ~~(Intervention Model for Air Pollution). Earth, Space and Environmental Chemistry (preprinted), 2021.~~

719 Thind, M. P. S.; Tessum, C. W.; Azevedo, I. L.; Marshall, J. D., Fine Particulate Air Pollution from  
720 Electricity Generation in the US: Health Impacts by Race, Income, and Geography. Environmental  
721 Science & Technology, 53, (23), 14010-14019, 2019.

722 United States Environmental Protection Agency. National Emission Inventory data.  
723 <https://www.epa.gov/air-emissions-inventories/2011-national-emissions-inventory-nei-data>. 2011.

724 Whitten G Z, Heo G, Kimura Y, et al. A new condensed toluene mechanism for Carbon Bond CB05-TU.  
725 Atmospheric Environment, 44(40SI):5346-5355, 2010.

726 Wu, R.; Liu, F.; Tong, D.; Zheng, Y.; Lei, Y.; Hong, C.; Li, M.; Liu, J.; Zheng, B.; Bo, Y.; Chen, X.; Li,  
727 X.; Zhang, Q., Air quality and health benefits of China's emission control policies on coal-fired power  
728 plants during 2005–2020. Environmental Research Letters, 14, (9), 094016, 2019.

729 Xiao, Q. Y.; Geng, G. N.; Liang, F. C.; Wang, X.; Lv, Z.; Lei, Y.; Huang, X. M.; Zhang, Q.; Liu, Y.; He,  
730 K., Changes in spatial patterns of PM<sub>2.5</sub> pollution in China 2000–2018: Impact of clean air policies.  
731 Environment international, 141, 105776, 2020.

732 Zhang, L.; Liu, L. C.; Zhao, Y. H.; Gong, S. L.; Zhang, X. Y.; Henze, D. K.; Capps, S. L.; Fu, T. M.;  
733 Zhang, Q.; Wang, Y. X., Source attribution of particulate matter pollution over North China with the  
734 adjoint method. Environmental Research Letters, 10, (8), 2015.

735 Zhang, Q.; Zheng, Y.; Tong, D.; Shao, M.; Wang, S.; Zhang, Y.; Xu, X.; Wang, J.; He, H.; Liu, W.; Ding,  
736 Y.; Lei, Y.; Li, J.; Wang, Z.; Zhang, X.; Wang, Y.; Cheng, J.; Liu, Y.; Shi, Q.; Yan, L.; Geng, G.; Hong,  
737 C.; Li, M.; Liu, F.; Zheng, B.; Cao, J.; Ding, A.; Gao, J.; Fu, Q.; Huo, J.; Liu, B.; Liu, Z.; Yang, F.; He,  
738 K.; Hao, J., Drivers of improved PM<sub>2.5</sub> air quality in China from 2013 to 2017. Proceedings of the  
739 National Academy of Sciences of the United States of America, 116, (49), 24463-24469, 2019.

740 Zheng, B.; Zhang, Q.; Zhang, Y.; He, K. B.; Wang, K.; Zheng, G. J.; Duan, F. K.; Ma, Y. L.; Kimoto, T.,  
741 Heterogeneous chemistry: a mechanism missing in current models to explain secondary inorganic aerosol

带格式的: 字体:(默认) Times New Roman, 10 pt,  
字体颜色: 文字 1, 不检查拼写或语法

带格式的: 字体:(默认) Times New Roman, 10 pt,  
字体颜色: 文字 1, 不检查拼写或语法

带格式的: EndNote Bibliography

带格式的: 字体:(默认) Times New Roman, 10 pt,  
字体颜色: 文字 1, 不检查拼写或语法

带格式的: 字体:(默认) Times New Roman, 10 pt,  
字体颜色: 文字 1, 不检查拼写或语法

带格式的: 字体:(默认) Times New Roman, 10 pt,  
字体颜色: 文字 1, 不检查拼写或语法

带格式的: 字体:(默认) Times New Roman, 10 pt,  
字体颜色: 文字 1, 不检查拼写或语法

带格式的: 字体:(默认) Times New Roman, 10 pt,  
字体颜色: 文字 1, 不检查拼写或语法

带格式的: 字体:(默认) Times New Roman, 10 pt,  
字体颜色: 文字 1, 不检查拼写或语法

带格式的: 字体:10 pt, 字体颜色: 文字 1,  
不检查拼写或语法

删除的内容:

743 formation during the January 2013 haze episode in North China. *Atmospheric Chemistry and Physics*,  
744 15, (4), 2031-2049, 2015.

745

746

747

748

749

750

751

752

753

754

755

756

757

758

759

760

761

762

763

764

765

766

767

768

769

770

771 **Table 1. Model configurations in InMAP-China.**

Category	Parameters	Configurations
Basic	Research area and period	China, 2017
	Spatial resolution	36 km × 36 km
	Vertical layers	14 layers
	Run type	Steady run
	Variable grid	Static grid
	Projection	Lambert
	Grid numbers	305816
	Meteorological and chemical parameters	Calculated using variables from WRFv3.8-CMAQv5.2
Input	Anthropogenic emissions	MEIC, MIX, MEGAN
	Population data	GPW 2015 and GBD 2017
	Baseline mortality rate	GBD 2017
Output	Air pollutants	PM <sub>2.5</sub> and its composition concentrations
	Mortality	PM <sub>2.5</sub> -related premature mortality

772

773

774

775

776

777

778

779

780

781

Table 2 The relationship between parameters for simplified simulation and original variables.

带格式表格

WRF-CMAQ's Variables	Descriptions	InMAP-China's Parameters	Descriptions
U, V, W	Wind fields	UAvg, UDeviation VAvg, VDeviation WAvg, WDeviation	Advection and mixing coefficients
PH, PHB	Base state of geopotential and perturbation geopotential	Dz	Layer heights
PBLH	Planetary boundary layer height	M2d, M2u, Kxxyy, Kzz	Mixing coefficients
T	Potential Temperature	SO <sub>2</sub> Oxidation, PlumeHeight	Chemical reaction rates and plume rise
P, PB	Base state pressure plus perturbation pressure		Chemical reaction rates and plume rise
QRAIN	Mixing ratio of rain	ParticleWetdep, GasWetdep	Wet deposition
QCLOUD	Cloud mixing ratio	SO <sub>2</sub> Oxidation	Aqueous-phase chemical reaction rates
CLDFRA	Fraction of grid cell covered by clouds	ParticleWetdep, GasWetdep	Wet deposition
SWDOW N, GLW	Downward shortwave and longwave radiative flux at ground level	GasDrydep, ParticleWetdep	Dry deposition
HFX	Surface heat flux	M2d, M2u, Kxxyy, Kzz, Drydep	Mixing and dry deposition
UST	Friction velocity		Mixing and dry deposition
LU_INDE X	Land use type	M2d, M2u, Kxxyy, Kzz	Mixing
DENS	Inverse air density		Mixing and convert between mixing ratio and mass concentration
aVOC	Anthropogenic VOCs that are SOA precursors	aOrgPartitioning	VOCs/SOA partitioning
aSOA	Anthropogenic SOA		
OH, H <sub>2</sub> O <sub>2</sub>	Hydroxyl radical and hydrogen peroxide concentrations	SO <sub>2</sub> Oxidation	Oxidation rates
pNO	ANO <sub>3</sub> I, ANO <sub>3</sub> J	NOPartitioning	

gNO	NO and NO <sub>2</sub>		NO <sub>x</sub> /pNO <sub>3</sub> partitioning
pNH	ANH <sub>4</sub> I, ANH <sub>4</sub> J	NHPartitioning	NH <sub>3</sub> /pNH <sub>4</sub> partitioning
gNH	NH <sub>3</sub>		

783

784

785

786

787

788

789

790

791

792

793

794

795

796

797

798

799

800

801

802

803

804

805

806

删除的内容:



809 **Table 3 Simulation experiments conducted using InMAP-China.**

Class	Simulations	Emission input	Physical and chemical parameter input
<u>Base</u>	<u>InMAP_TOT</u>	<u>Five sectoral anthropogenic emissions and natural emissions</u>	
<u>High re</u>	<u>InMAP_BTH</u>	<u>Five sectoral anthropogenic emissions and natural emissions with 4km resolution at BTH region</u>	
Sec1	InMAP_POW	Power plants emissions	
Sec2	InMAP_INDUS	Industrial emissions	
Sec3	InMAP_TRANS	Transportation emissions	
Sec4	InMAP_RESI	Residential emissions	
Sec5	InMAP_AGRI	Agricultural emissions	
Aba1	InMAP_RE10	Reduce the air pollutants emissions by 10% based on InMAP_TOT emissions	
Aba2	InMAP_RE30	Reduce the air pollutants emissions by 30% based on InMAP_TOT emissions	Converted using WRF-CMAQv5.2 simulation data in the year of 2017;
Aba3	InMAP_RE50	Reduce the air pollutants emissions by 50% based on InMAP_TOT emissions	Remain the same in all simulations.
Aba4	InMAP_RE70	Reduce the air pollutants emissions by 70% based on InMAP_TOT emissions	
Aba5	InMAP_RE90	Reduce the air pollutants emissions by 90% based on InMAP_TOT emissions	

删除的内容:

删除的内容: BASE

删除的内容: InMAP\_TOT

删除的内容: Five sectoral anthropogenic emissions and natural emissions

删除的内容: CMAQv5.2

810  
811  
812  
813  
814  
815  
816  
817

825

Table 4 Comparison of the proportions of sectoral contributions to PM<sub>2.5</sub> concentrations using InMAP-

删除的内容:

826 China and CMAQ.

Sector	National		BTH		YRD		PRD		FWPY	
	CMAQ	InMAP-China	CMAQ	InMAP-China	CMAQ	InMAP-China	CMAQ	InMAP-China	CMAQ	InMAP-China
Power	6.9%	8.1%	6.2%	9.4%	7.4%	8.6%	10.4%	8.2%	7.0%	10.0%
Industry	30.8%	35.0%	30.2%	38.2%	33.3%	39.1%	37.5%	35.4%	27.7%	31.9%
Residential	25.9%	28.1%	24.7%	28.2%	17.9%	20.8%	19.5%	28.4%	30.0%	33.8%
Transportation	14.0%	17.3%	13.4%	15.6%	15.7%	21.2%	17.1%	17.5%	13.2%	15.0%
Agriculture	22.5%	11.5%	25.5%	10.4%	25.7%	12.4%	15.4%	11.6%	22.0%	9.4%

827

828

829

830

831

832

833

834

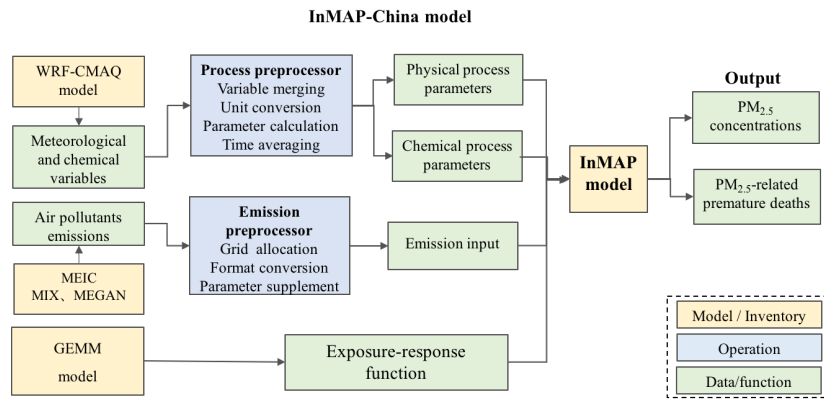
835

836

837

838

839



841

842

**Figure 1 Model framework of InMAP-China.**

843

844

845

846

847

848

849

850

851

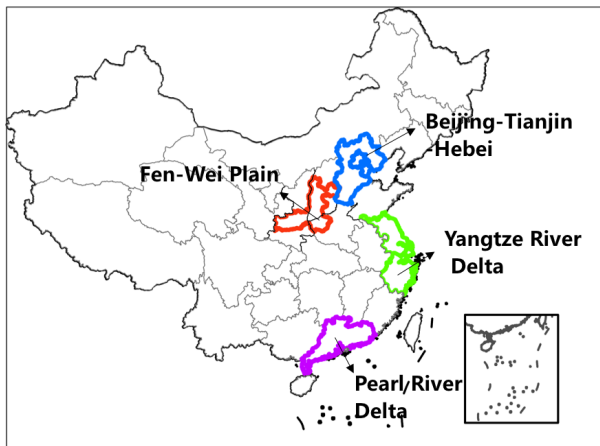
852

853

854

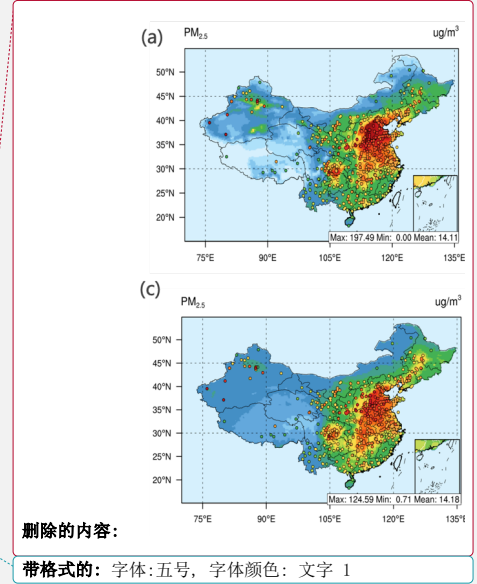
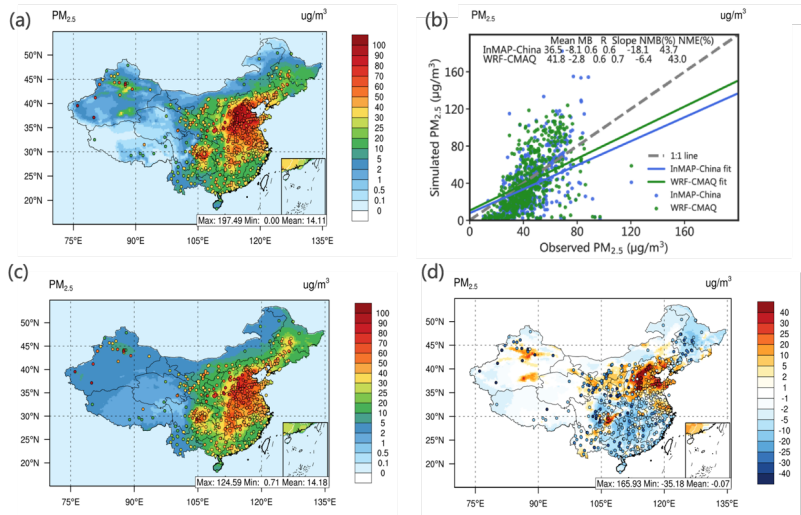
855

856

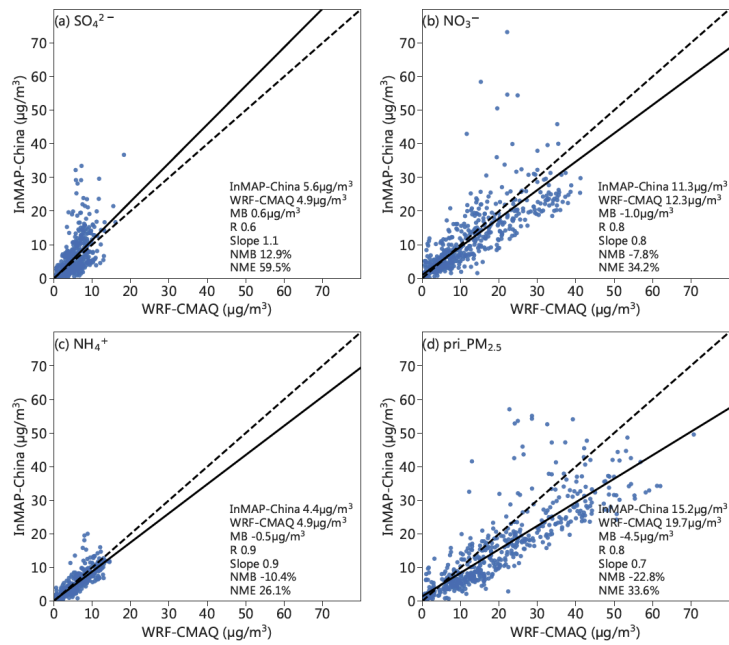


857  
858 **Figure 2** Four key regions defined in this study, including the Beijing-Tianjin-Hebei region, Yangtze River  
859 Delta region, Pearl River Delta region and Fen Wei Plain region.

860  
861  
862  
863  
864  
865  
866  
867  
868  
869  
870



871  
872 **Figure 3 The spatial pattern and statistical metrics of total PM<sub>2.5</sub> concentrations predicted by InMAP-China**  
873 **and WRF-CMAQ.** Panels (a) and (c) display the spatial patterns of total PM<sub>2.5</sub> concentrations predicted by InMAP-  
874 China and WRF-CMAQ, respectively. Panel (d) presents the difference in the spatial distribution of the total PM<sub>2.5</sub>  
875 concentrations predicted by the two models. Panel (b) shows the statistical metrics between the simulated and  
876 observed PM<sub>2.5</sub>. The observed total PM<sub>2.5</sub> concentrations are marked as circles in panel (a) and panel (c). In panel  
877 (d), the circle shows the difference between the PM<sub>2.5</sub> simulated by InMAP-China and the observed PM<sub>2.5</sub>. The same  
878 colorbar is utilized in the contour and the marked circle.



880

881

**Figure 4** Scatter plot comparing the PM<sub>2.5</sub> composition concentration modelled by the InMAP-China and

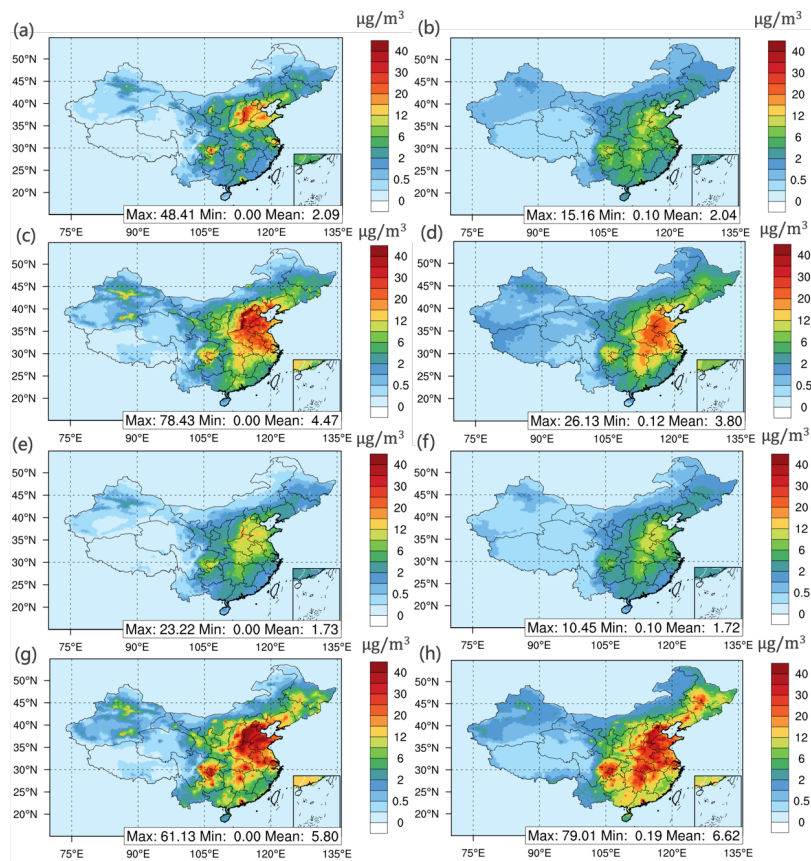
882

**WRF-CMAQ** models. Panels (a), (b), (c) and (d) display sulfate, nitrate, ammonium, and primary PM<sub>2.5</sub>,

883

respectively. The statistical metrics are labelled in the lower right corner of each panel.

删除的内容: in

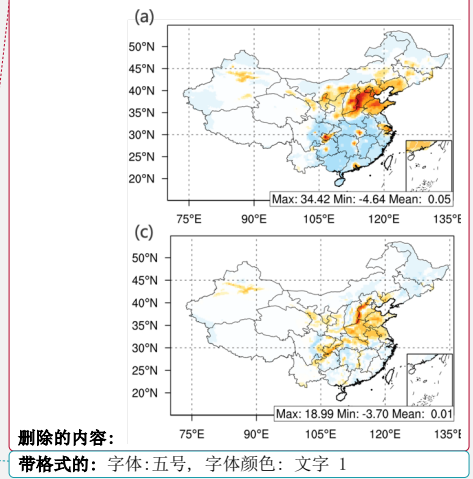
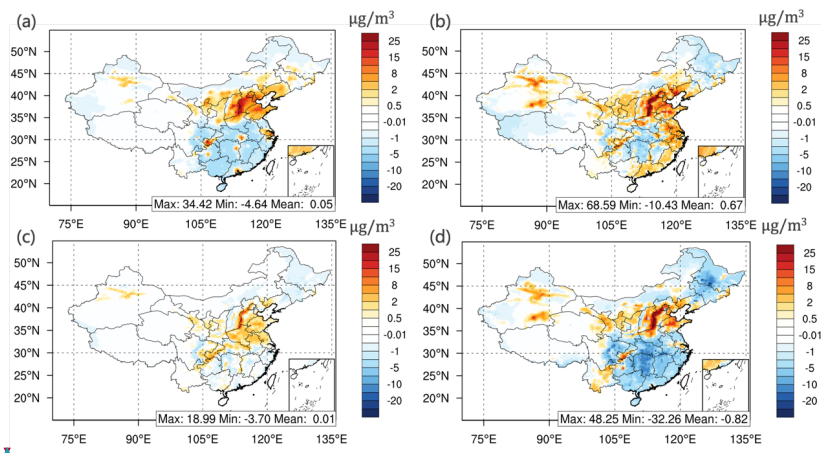


885

886 **Figure 5** The spatial pattern of PM<sub>2.5</sub> compositions modelled by the InMAP-China and WRF-CMAQ models.

887 Panels (a), (c), (e), and (g) present the sulfate, nitrate, ammonium, and primary PM<sub>2.5</sub>, respectively, simulated by

888 InMAP-China in the InMAP-TOT scenario. Panels (b), (d), (f), and (h) present the results modelled by WRF-CMAQ.



889

890 **Figure 6** The difference in the spatial pattern of PM<sub>2.5</sub> compositions between InMAP-China and WRF-CMAQ.

891 Panels (a), (b), (c), and (d) display sulfate, nitrate, ammonium, and primary PM<sub>2.5</sub>, respectively.

892

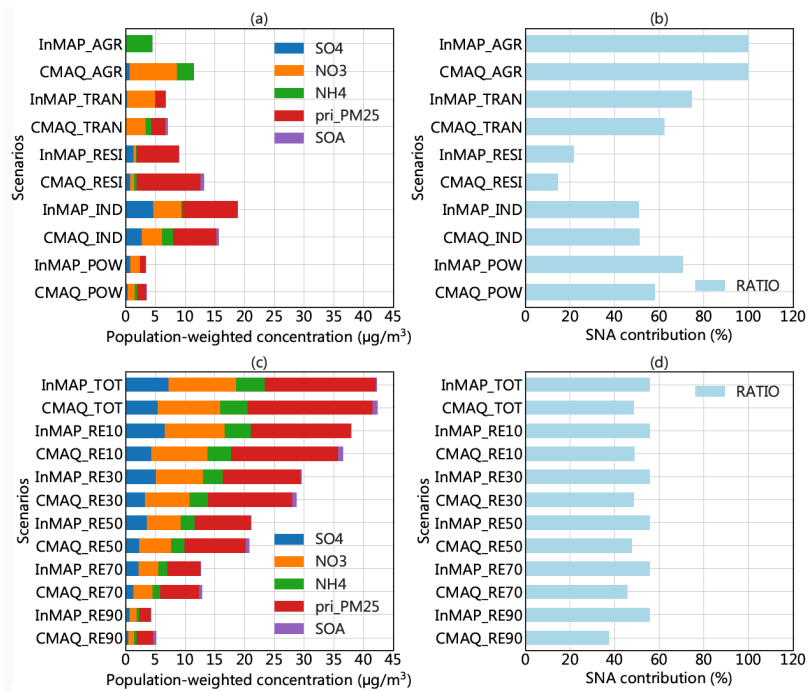
893

894

895

896





898

899

**Figure 7 Comparison of PM<sub>2.5</sub> component concentrations and SNA contributions in these eleven simulations.**

900

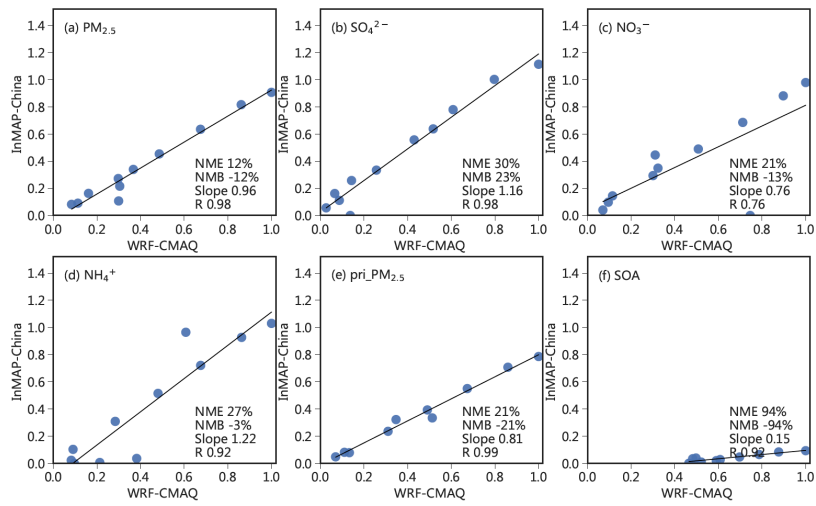
(a) and (c) show the modelled PM<sub>2.5</sub> compositions. Panel (a) presents the results of sectoral emission scenarios, and

901

panel (c) presents the results of the baseline and emission abatement scenarios. Panels (b) and (d) present the SNA

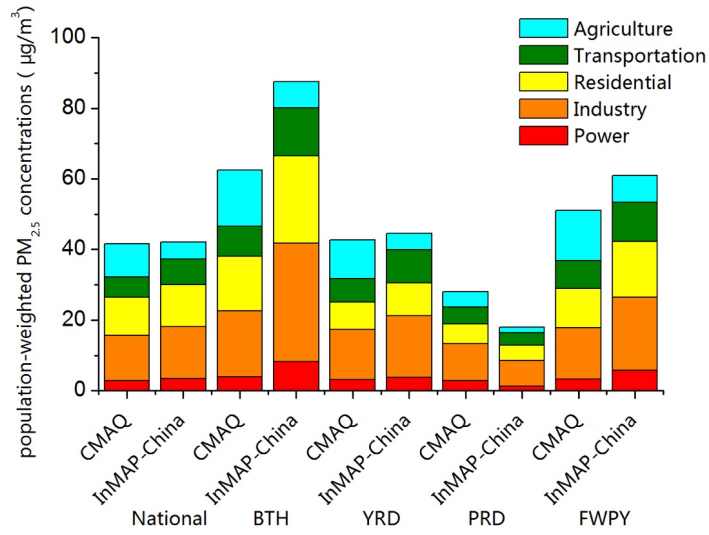
902

contribution (%) for each scenario.



903  
 904 **Figure 8 Marginal change in nationwide annual average population-weighted  $PM_{2.5}$  concentration and its**  
 905 **composition as modelled by InMAP-China and WRF-CMAQ for eleven emissions scenarios.** The population-  
 906 weighted pollutant concentration for each scenario is normalized using the largest value among all scenarios  
 907 modelled by CMAQ. The eleven dots represent the eleven scenarios, and the statistical metrics are labelled in the  
 908 lower right corner for each panel.

909  
 910  
 911



912

913 **Figure 9 Comparison of source contributions to population-weighted PM<sub>2.5</sub> concentrations estimated by the**

914 **two models.**

915

916

917

918

919

920

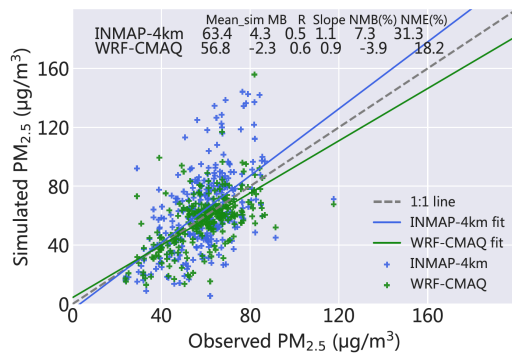
921

922

923

924

带格式的: 正文



带格式的: 居中

删除的内容: .

Figure

带格式的: 字体:五号, 字体颜色: 文字 1

925

926

927

928

929

930

931

932

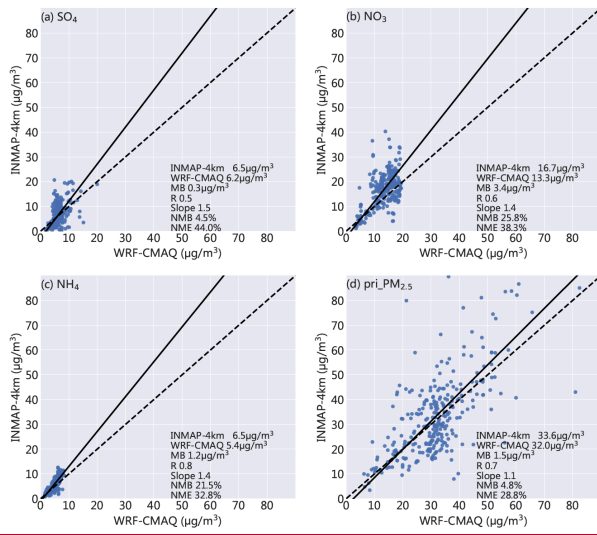
933

934

935

936

**Figure 10 Scatter plot comparing the PM<sub>2.5</sub> concentration modeled in the BTH region with 4 km spatial resolution by the InMAP-China and WRF-CMAQ. The value of statistical metrics is labeled in the panel.**



带格式的: 字体:小五, 字体颜色: 文字 1

带格式的: 居中

939

940 **Figure 11 Scatter plot comparing the PM<sub>2.5</sub> composition concentration modeled at BTH region with 4km**

941 **spatial resolution by the InMAP-China and WRF-CMAQ. Panels (a), (b), (c) and (d) display the sulfate, nitrate,**

942 **ammonium, and primary PM<sub>2.5</sub>, respectively. The statistical metrics are labeled in the lower right corner of each**

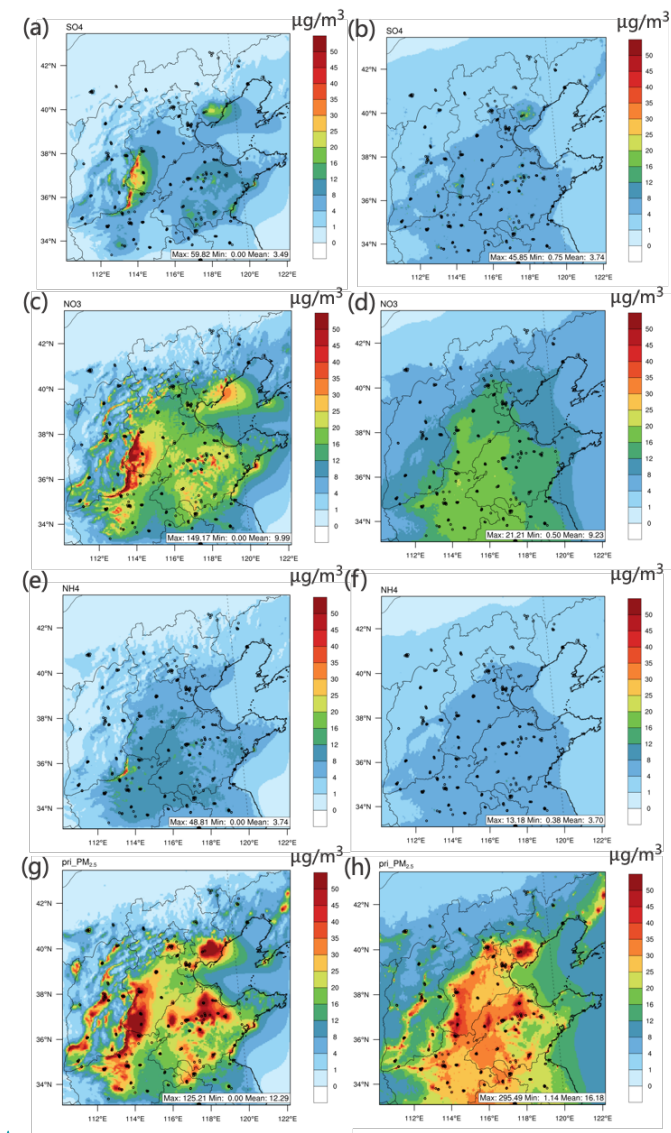
943 **panel.**

944

带格式的: 英语(英国)

945

带格式的: 居中



带格式的: 字体:小五, 字体颜色: 文字 1

带格式的: 两端对齐

删除的内容:

带格式的: 检查拼写和语法

带格式的: 英语(美国)

946

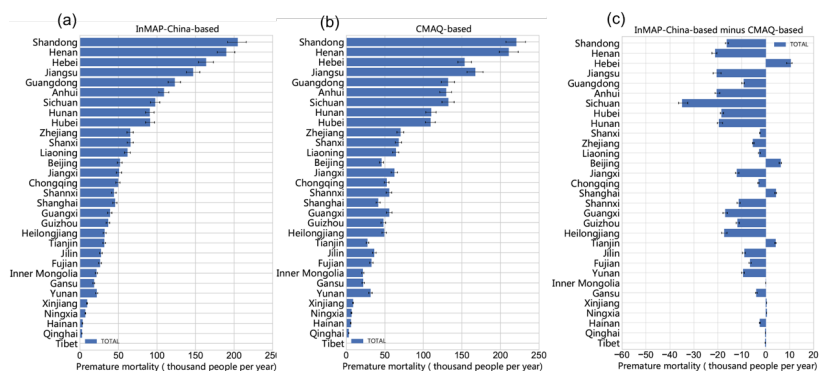
947

948

949

950

**Figure 12** The spatial pattern of  $PM_{2.5}$  compositions simulated in the BTH region with 4km spatial resolution by the InMAP-China and WRF-CMAQ. Panels (a), (c), (e), and (g) present the sulfate, nitrate, ammonium, and primary  $PM_{2.5}$ , respectively, simulated by InMAP-China. Panels (b), (d), (f), and (h) present the corresponding results simulated by WRF-CMAQ.



带格式的: 字体:五号, 字体颜色: 文字 1

953  
954  
955  
956  
957  
958  
959  
960  
961  
962  
963  
964

Figure 13 Comparison of PM<sub>2.5</sub>-related premature mortality using the PM<sub>2.5</sub> predictions from two models.

带格式的: 下标

(a) InMAP-China-based; (b) CMAQ-based; and (c) difference between the two models.

带格式的: 英语(美国)